EDGE ARTICLE

CrossMark
click for updates

HKOCl-3: a fluorescent hypochlorous acid probe for live-cell and *in vivo* imaging and quantitative application in flow cytometry and a 96-well microplate assay†

Jun Jacob Hu,‡[a] Nai-Kei Wong,‡[a] Ming-Yang Lu,[a] Xingmiao Chen,[b] Sen Ye,[a] Angela Qian Zhao,[a] Peng Gao,[c] Richard Yi-Tsun Kao,[c] Jiangang Shen[b] and Dan Yang*[a]

Ultra-selective and ultra-sensitive probes for hypochlorous acid (HOCl), one of the most poorly understood reactive oxygen species (ROS), are urgently needed to unravel the HOCl functions in important biological processes such as development and innate immunity. Based on a selective oxidative *O*-dearylation reaction of 2,6-dichlorophenol toward HOCl over other reactive oxygen species, we have developed a novel fluorescent probe **HKOCl-3** for HOCl detection with ultra-selectivity, ultra-sensitivity and a rapid turn-on response. The functional robustness of **HKOCl-3** for endogenous HOCl detection and imaging has been thoroughly scrutinized in multiple types of phagocytes and *in vivo* imaging of live intact zebrafish embryos. Furthermore, **HKOCl-3** has been successfully applied to the detection of endogenous HOCl by a 96-well microplate assay and flow cytometry. Therefore, **HKOCl-3** holds great promise as a versatile molecular tool that enables innovative investigation of HOCl biology and ROS-related diseases in multiple detection modalities.

Introduction

A wide spectrum of reactive oxygen/nitrogen species such as $O_2^{\cdot-}$, H_2O_2, $^{\cdot}NO$, HOCl and $ONOO^-$ form the chemical underpinnings of cellular life. Their actions are tied with diverse physiological and pathological conditions, *e.g.* development, aging, inflammation, autoimmunity, cancer and neurodegeneration.[1] In particular, HOCl, produced by the myeloperoxidase-catalyzed reaction of H_2O_2 with a chloride ion (Cl^-), has been reputed to be a key microbicidal effector in innate immunity.[2–4] Additionally, aberrant accumulation of HOCl in phagocytes can trigger tissue damage or remodeling, with profound implications for many human diseases including cardiovascular diseases,[5] inflammatory diseases,[6] acute lung injuries,[7] nephropathies,[8] cystic fibrosis,[9] neurodegenerative disorders,[10] and certain cancers.[11]

The past decade has witnessed tremendous efforts toward the development of fluorescent probes for HOCl imaging and detection, based on distinct strategies.[12] However, a lack of suitable fluorescent probes for selective and sensitive HOCl detection in quantitative platforms such as flow cytometry and 96-well microplate assays has seriously impeded advances in understanding the roles of HOCl in various biological processes. To meet the demands of intricate biological studies, especially for quantitative detection in cells, highly versatile and robust HOCl probes with ultra-selectivity (*i.e.* >50-fold more sensitive toward HOCl than other reactive oxygen/nitrogen species), ultra-sensitivity (*i.e.* >100-fold enhancement toward 1 equiv. HOCl) and a rapid turn-on response (*i.e.* <1 min) need to be developed.[13]

Here we report the development of a novel HOCl fluorescent probe **HKOCl-3** with ultra-selectivity, ultra-sensitivity and a rapid turn-on response for live-cell and *in vivo* imaging and quantitative application in flow cytometry and a 96-well microplate assay.

[a]*Morningside Laboratory for Chemical Biology and Department of Chemistry, The University of Hong Kong, Pokfulam Road, Hong Kong, P. R. China. E-mail: yangdan@hku.hk*

[b]*School of Chinese Medicine, The University of Hong Kong, Pokfulam Road, Hong Kong, P. R. China*

[c]*Department of Microbiology, Research Center of Infection and Immunology and State Key Laboratory of Emerging Infectious Diseases, Pokfulam Road, Hong Kong, P. R. China*

† Electronic supplementary information (ESI) available: Experimental procedures, characterization data and additional spectra. See DOI: 10.1039/c5sc03855c

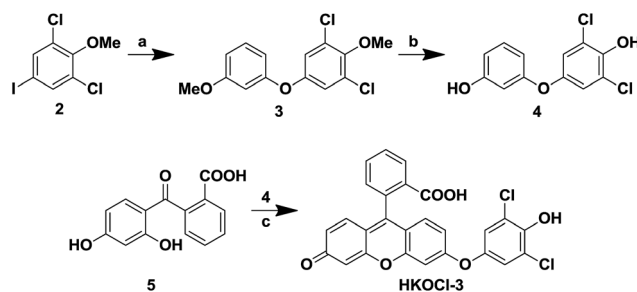‡ These authors contribute equally to this work.

Results and discussion

Design and synthesis of the fluorescent probe HKOCl-3

A widely used fluorescent probe HPF, reported by Nagano and coworkers,[12a] shows a strong response toward $^{\cdot}OH$ and $ONOO^-$,

but not HOCl. As part of our continued efforts in developing fluorescent probes for the detection of specific reactive oxygen species,[14] we noticed that, by incorporating *ortho* halogen substituents, the selectivity of the resulting phenols toward HOCl over other reactive oxygen/nitrogen species can be dramatically improved. Therefore, we designed a new fluorescent probe **HKOCl-3** (Scheme 1) by incorporating two *ortho* chlorine substituents into HPF. Since the introduction of two chlorine atoms (2,6-dichlorophenol moiety) lowers the pK_a of the phenol by more than 3 orders of magnitude (from 10.0 to 6.79), the election-rich phenoxide form of **HKOCl-3** will be dominant under physiological conditions (pH = 7.4), resulting in a great enhancement of its nucleophilicity and reactivity toward HOCl. In addition, the phenoxide form of **HKOCl-3** can quench the fluorescence by a photoinduced electron transfer (PeT) process more efficiently, affording lower basal fluorescence. Herein, we report that **HKOCl-3** is indeed an excellent fluorescent probe for HOCl detection with ultra-selectivity, ultra-sensitivity and a rapid turn-on response in live cells and *in vivo*.

As shown in Scheme 2, the probe **HKOCl-3** was readily synthesized from diarylether **4** (obtained by Ullmann coupling of 3-methoxyphenol and aryl iodide **2**, followed by demethylation) and benzoic acid **5** (prepared from fluorescein) in a good yield.

Reactivity and selectivity of HKOCl-3 for HOCl

For chemical characterization, we first investigated the spectroscopic properties of the fluorescent probe **HKOCl-3** (10 μM) in potassium phosphate buffer (0.1 M, pH 7.4, 0.1% DMF) at 25 °C. **HKOCl-3** showed an obvious absorption peak at 455 nm ($\varepsilon = 2.3 \times 10^4$ M^{-1} cm^{-1}; Fig. S1†), and as expected, its fluorescence is completely quenched ($\Phi = 0.001$). Upon exposure to 1 equiv. HOCl, a >358-fold enhancement in the fluorescence intensity was observed, demonstrating the ultra-sensitivity of this probe in aqueous solution (Fig. 1a). A linear relationship of the fluorescence intensity of **HKOCl-3** at 527 nm with the concentrations of HOCl (0–10 μM) was observed (Fig. 1b). Moreover, the detection limit of **HKOCl-3** was calculated to be as low as 0.33 nM ($3\sigma/k$). This again confirms the ultrasensitivity of **HKOCl-3**, compared with the previously reported HOCl probes. In particular, the reaction of **HKOCl-3** (10 μM) with HOCl caused
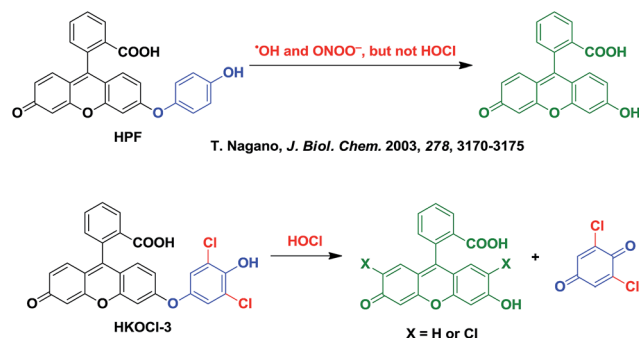

Scheme 2 Synthesis of the fluorescent probe **HKOCl-3**. Reagents and conditions: (a) CuI, *N,N*-dimethylglycine hydrochloride, Cs$_2$CO$_3$, dioxane, 90 °C 24 h, 81%; (b) HBr (48 wt%), AcOH, reflux, 12 h, 91%; (c) TFA, 100 °C, 12 h, 61%.

a dramatic time-dependent fluorescence increase, which was complete within 1 min (Fig. 1c), suggesting a remarkably fast reaction between the probe and HOCl.

Interestingly, upon treatment with HOCl, **HKOCl-3** underwent a bathochromic shift in the absorption peak (from 455 nm to 499 nm, Fig. S1, ESI†) and fluorescence emission peak (Fig. 1a and S2, ESI†). This indicates that the oxidation of **HKOCl-3** produced fluorescent products, such as fluorescein and its mono- or di-chlorinated derivatives (Scheme 1), which have been confirmed by ESI-MS analysis (ESI†). Moreover, the fluorescence signal remained unchanged for 30 min (Fig. S3, ESI†), indicating the striking chemo-stability of the fluorescent products toward the highly reactive HOCl in the reaction mixture.

Next, the selectivity of **HKOCl-3** was examined by measuring its fluorescence response upon treatment with various analytes

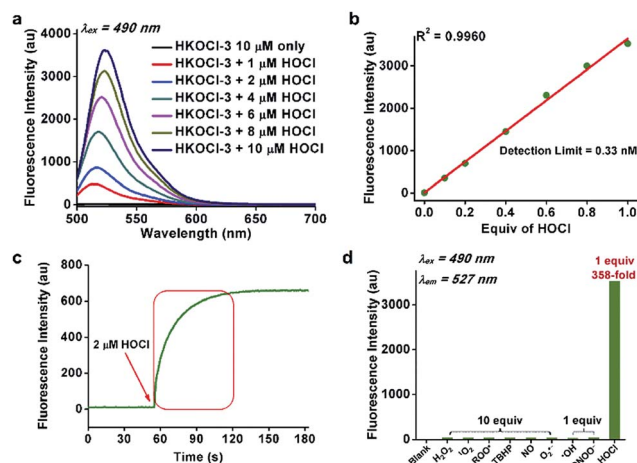**Scheme 1** Design of the new fluorescent probe **HKOCl-3**.

Fig. 1 Characterization of **HKOCl-3** performance in chemical systems. The fluorescent probe **HKOCl-3** was dissolved in 0.1 M potassium phosphate buffer at pH 7.4 to a final concentration of 10 μM (containing 0.1% DMF). (a) Fluorescence emission spectra of the fluorescent probe **HKOCl-3** upon treatment with different amounts of HOCl (0–10 μM); (b) fluorescence intensity of **HKOCl-3** (at 527 nm) as a function of HOCl (at 0–10 μM); (c) the time course of fluorescence intensity of **HKOCl-3** at 527 nm after treatment with 2 μM HOCl (time range 0–180 s); (d) fluorescence responses of the probe **HKOCl-3** toward various reactive oxygen/nitrogen species. The fluorescence spectra were recorded at 30 min with an excitation at 490 nm.

in potassium phosphate buffer (0.1 M, pH 7.4). As shown in Fig. 1d and Table S1 (ESI†), 1 equiv. of HOCl gave a >358-fold enhancement in fluorescence intensity, while 10 equiv. (100 μM) of other biologically relevant reactive oxygen/nitrogen species (H_2O_2, $^1O_2$, ROO$^•$, TBHP, $^•$NO and $O_2^{•-}$) only triggered a negligible fluorescence increase. Specifically, the probe exhibited a >83-fold higher increase in fluorescence intensity toward HOCl over other potentially interfering highly reactive oxygen species ($^•$OH and ONOO$^-$). Collectively, these results demonstrate the ultra-selectivity of **HKOCl-3** for HOCl.

The biocompatibilty of **HKOCl-3** was then examined. **HKOCl-3** exhibits an excellent stability toward pH changes (3.0–10.8, Fig. S4, ESI†) and its fluorescence response toward HOCl was significant across a wide range of pH values (4–10) relevant to cellular processes (Fig. S5, ESI†). The interference from common coexisting biological substances (Na^+, Ca^{2+}, Mg^{2+}, Zn^{2+}, glutathione, *etc.*) was found to be minimal (Fig. S6, ESI†). Collectively, these results suggest that the probe **HKOCl-3** could be used to detect HOCl reliably in complex cellular milieux.

Evaluation of HKOCl-3 for endogenous HOCl detection in live cells and *in vivo*

As a first step to establish the biological applications of **HKOCl-3**, the cytotoxicity of **HKOCl-3** was assessed in RAW264.7 mouse macrophages. **HKOCl-3** was found to be virtually nontoxic when used up to 20 μM after 24 h incubation (Fig. S7, ESI†). Then we examined the performance of this probe in confocal imaging of endogenous HOCl in different types of activated phagocytes: RAW264.7 mouse macrophages, BV-2 mouse microglia, THP-1 human monocytic macrophages[15] and primary human polymorphonuclear neutrophils (PMNs). To induce endogenous HOCl, different types of phagocytes were co-incubated with **HKOCl-3** (1 μM) and the PKC activator PMA (phorbol myristate acetate: 500 ng mL^{-1}) for 30 min, followed by confocal imaging (Fig. 2, S8 and S9, ESI†). As expected, unstimulated phagocytes loaded with **HKOCl-3** showed barely detectable background fluorescence signals (Fig. 2). In the presence of PMA, the fluorescence signal was significantly enhanced in all four types of cells. This result suggests that endogenous HOCl production can be robustly visualized with **HKOCl-3** in activated phagocytes.

The 96-well microplate fluorescence measurement is an indispensable platform for the development of low-cost, high-throughput screening assays, and is preferred over flow cytometry for its ability to preserve the physical integrity of live adherent cells during tests. However, the high background noise of 96-well microplate assays prohibits the successful application of numerous fluorescent probes, despite their excellent performance in chemical systems. To test the applicability of **HKOCl-3** in this platform, RAW264.7 mouse macrophages were co-incubated with **HKOCl-3** (2 μM) and various concentrations of PMA (0–1000 ng mL^{-1}) for 30 min before the fluorescence measurement. We found that **HKOCl-3** gave a dose-dependent response toward the PMA stimulation in RAW264.7 cells in a sensitive manner (Fig. 3a), which is in agreement with our confocal imaging results (Fig. S10, ESI†).
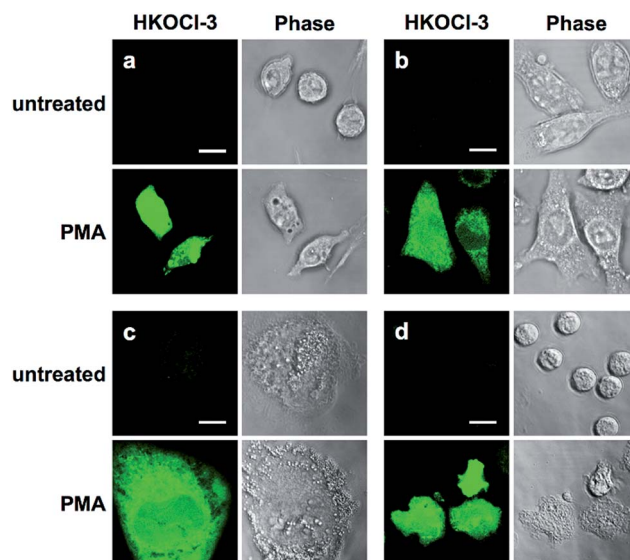

Fig. 2 Detection of endogenous HOCl by **HKOCl-3** in multiple cell types. Four types of phagocytes: RAW264.7 (a), BV-2 (b), differentiated THP-1 (c), and primary human PMN (d) cells were co-incubated with **HKOCl-3** (1 μM) with or without PMA (phorbol myristate acetate: 500 ng mL^{-1}), before confocal imaging. Scale bars represent 10 μm.

Next, the selectivity of **HKOCl-3** toward HOCl was thoroughly scrutinized by examining the effects of a series of enzyme inhibitors. RAW264.7 cells were co-incubated with **HKOCl-3** (2 μM) and PMA (500 ng mL^{-1}) in the presence or absence of one of the following inhibitors: the PKC inhibitors Gö6983, Gö6976 and Ro32-0432, the NOX (NADPH oxidase) inhibitor DPI (diphenyleneiodonium chloride), and the MPO (myeloperoxidase) inhibitor ABAH (aminobenzoic acid hydrazide). The observation that the fluorescence signal was potently and dose-dependently reduced by these inhibitors confirms the selectivity of **HKOCl-3** toward HOCl detection, as PKC and NOX are known to be upstream of MPO in the pathway for endogenous HOCl production in activated RAW264.7 cells (Fig. 3b, ESI†).

The 96-well microplate platform has also been applied to evaluate the HOCl scavenging efficiency of five organosulfur compounds, namely: α-lipoic acid (which participates in aerobic metabolism), NAC (*N*-acetylcysteine), L-methionine, L-cysteine, and L-cystine (Fig. 4 and S11, ESI†). Except for L-cystine, which is a dimeric form of oxidized L-cysteine with a very poor aqueous solubility (200 μM in HBSS), all scavengers in the mM range were able to remove the HOCl generated in cells, with the order of scavenging efficiency as follows: L-cysteine < L-methionine < α-lipoic acid < NAC. Therefore, for the first time, we quantitatively and directly evaluated the HOCl removal effects of these scavengers, which support the findings generated in cell-free systems or by indirect measurement.[16] To the best of our knowledge, **HKOCl-3** is the first small-molecule probe that can be successfully applied to a 96-well microplate assay and can screen for molecules that scavenge HOCl or modulate its production.

Flow cytometry has become a definitive quantitative cellular analysis technique that rapidly integrates information about
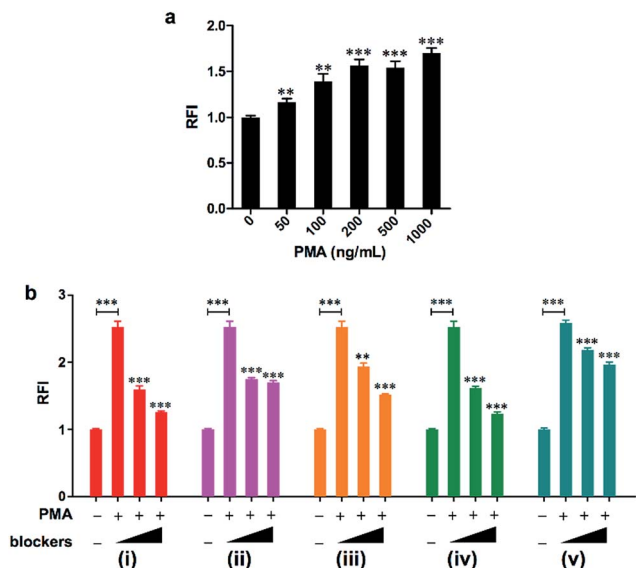
Fig. 3 Detection of endogenous HOCl with **HKOCl-3** in a 96-well microplate assay. (a) Dose-dependent **HKOCl-3** fluorescence changes in response to PMA in RAW264.7 cells. The fluorescence intensity of **HKOCl-3** (2 μM) after the 30 min PMA challenge was measured. (b) Validation of the **HKOCl-3** selectivity in PMA-stimulated RAW264.7 cells in the presence of various enzyme inhibitors. The probe (2 μM) and inhibitors were co-incubated for 30 min before measurement. (i) Gö6983 (0, 25 and 100 nM); (ii) Gö6976 (0, 25 and 100 nM); (iii) Ro32-0432 (0, 25 and 100 nM); (iv) DPI (0, 10 and 50 nM); (v) ABAH (0, 50 and 200 μM). Results are representative of at least three independent experiments. RFI: relative fluorescence intensity.
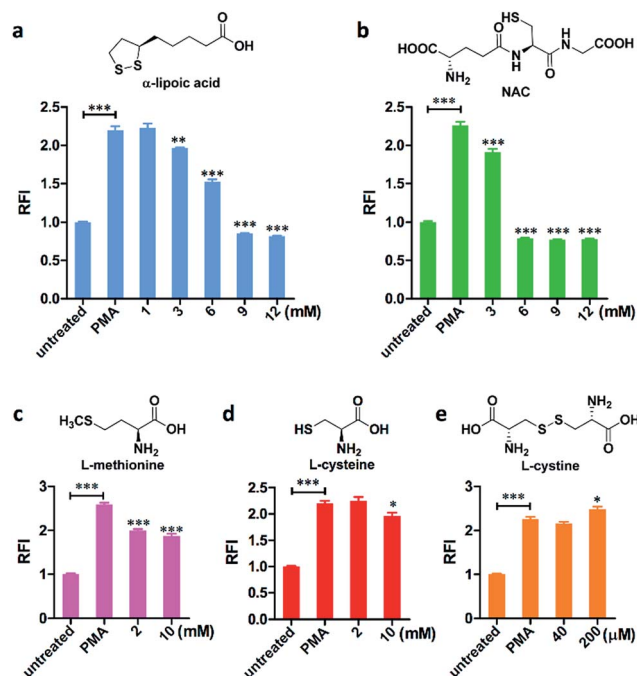

Fig. 4 Screening of HOCl scavengers with **HKOCl-3** in a 96-well microplate assay. RAW264.7 cells were co-incubated with **HKOCl-3** (2 μM) and PMA (500 ng mL^{-1}), in the absence or presence of the HOCl scavengers: (a) α-lipoic acid, (b) NAC, (c) L-methionine, (d) L-cysteine, and (e) L-cystine (at the indicated doses) for 30 min, before a 96-well microplate analysis. Results are representative of at least three independent experiments.

the multifaceted characteristics of cell populations (*e.g.* 10^3 cells per second). Based on the superb probe performance seen in confocal imaging and the 96-well microplate assay, we decided to explore the application of **HKOCl-3** in flow cytometry. RAW264.7 cells were co-incubated with **HKOCl-3** (2 μM) and PMA (500 ng mL^{-1}) in the presence or absence of the NOX inhibitor DPI (100 nM) for 30 min, followed by flow cytometry analysis (Fig. 5). In the presence of PMA, the geometric mean of the fluorescence intensity was significantly elevated. The appearance of two populations of cells upon the PMA challenge is an interesting and highly reproducible phenomenon in this assay, which could be explained by the distinct excitability or responsiveness of cell subpopulations (possibly under a different cellular redox status) toward PMA treatment. In addition, DPI blunted this fluorescence increase to a great extent. This result demonstrates that endogenous HOCl production in RAW264.7 cells can be readily detected in flow cytometry by using **HKOCl-3** as a fluorescent probe.

For decades, MPO-related oxidative damage in diverse inflammatory, vascular and neurodegenerative diseases has been reported in numerous studies, which vividly illustrates the functional relevance of HOCl in cardiovascular and nervous systems and the dire consequences of its dysregulated production.[17] Despite the well-documented pathological roles of HOCl in tissue damage, virtually nothing is known of HOCl function in normal tissues, such as those in developing fetuses. Strikingly, in zebrafish, an excellent *in vivo* model for studying the
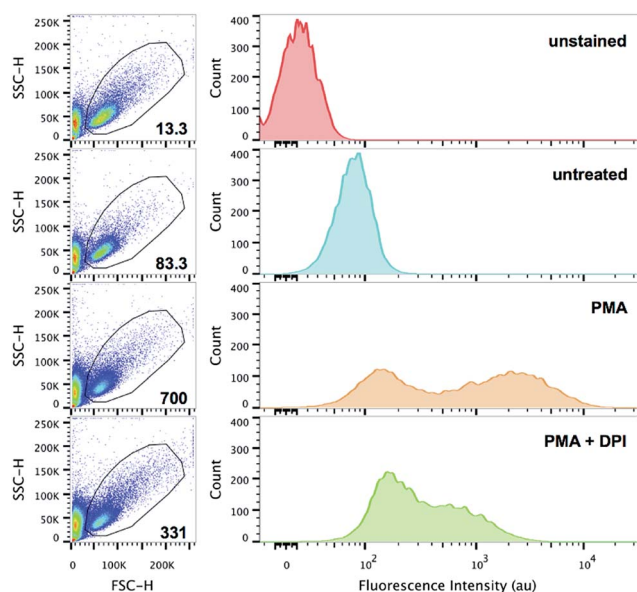

Fig. 5 Detection of endogenous HOCl in flow cytometry with **HKOCl-3**. RAW264.7 cells were co-incubated with **HKOCl-3** (2 μM) with or without PMA (500 ng mL^{-1}) and DPI (100 nM) for 30 min and analyzed by flow cytometry. The numbers in the dot plots represent the geometric means of fluorescence intensity. Results are representative of at least three independent experiments.
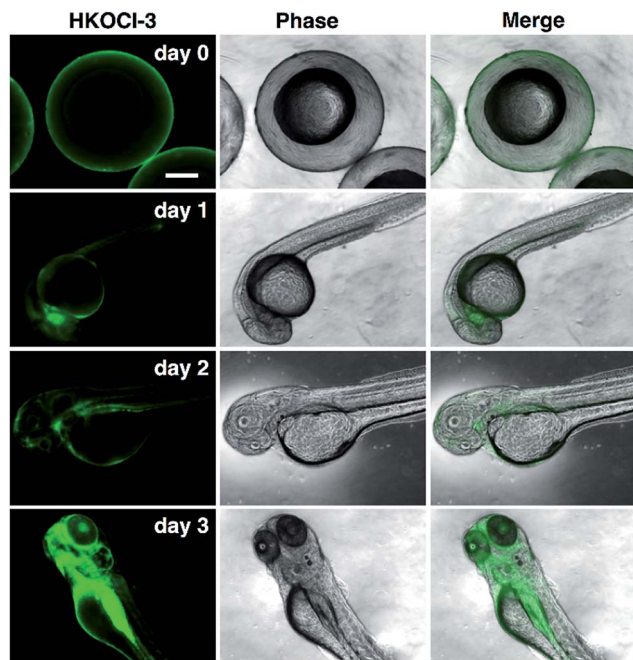
Fig. 6 Imaging of endogenous HOCl in live intact zebrafish embryos on different post-fertilization days. Zebrafish embryos ($n = 6$) at the indicated time of harvest were incubated with **HKOCl-3** (10 µM) in an E3 buffer for 30 min, before imaging at a low magnification (10×). Merge: the fluorescence and phase images merged. Scale bar represents 250 µm.

hematopoiesis and maturation of the immune system, the transcriptional expression of MPO has been known to occur in the very early stages of development (*e.g.* post-fertilization, day 1).[18] Yet the nature and distribution of the MPO activity (monitored through HOCl production) remains unclear. To this end, we sought to apply our probe **HKOCl-3** to visualize the endogenous HOCl in live intact zebrafish embryos at different developmental stages. Briefly, wild-type zebrafish embryos were harvested on 1–3 post-fertilization days (pfd). The embryos were incubated with **HKOCl-3** (10 µM) for 30 min and imaged under a fluorescence microscope. An intriguing pattern of progressively more intense and localized HOCl production in the live intact zebrafish embryos was observed (Fig. 6), which parallels the evolving complexity of the tissue differentiation during 1–3 pfd. Hence **HKOCl-3** can be readily applied to profile the distribution of the MPO activity in delicate live tissues in an ultra-sensitive and non-invasive manner.

Conclusions

As a strong oxidant with broad-spectrum reactivity toward multiple biomolecules, HOCl has been among the most mysterious reactive oxygen species in biology. To provide powerful tools for the investigation of HOCl biology, in this study we have successfully developed a new ultra-selective, ultra-sensitive and rapid turn-on fluorescent probe **HKOCl-3** for the molecular imaging and quantitative detection of HOCl. Specifically, the functional robustness of **HKOCl-3** has been established by visualizing endogenous HOCl in multiple living phagocytes in an oxidative burst model and in the *in vivo* imaging of live zebrafish embryos at different developmental stages. In addition, **HKOCl-3** has shown superior sensitivity in the quantitative detection of endogenous HOCl in flow cytometry and a 96-well microplate assay. Collectively, our probe is expected to offer exciting glimpses into the unknown roles of HOCl in cellular processes and to help accelerate discoveries of drugs for the treatment of human diseases.

Notes and references

1 C. C. Winterbourn, *Nat. Chem. Biol.*, 2008, **4**, 278–286.
2 F. C. Fang, *Nat. Rev. Microbiol.*, 2004, **2**, 820–832.
3 S. M. McKenna and K. J. Davies, *Biochem. J.*, 1988, **254**, 685–692.
4 D. Roos and C. C. Winterbourn, *Science*, 2002, **296**, 669–671.
5 L. J. Hazell, L. Arnold, D. Flowers, G. Waeg, E. Malle and R. Stocker, *J. Clin. Invest.*, 1996, **97**, 1535–1544.
6 C. C. Winterbourn and A. J. Kettle, *Free Radicals Biol. Med.*, 2000, **29**, 403–409.
7 S. Hammerschmidt, N. Buchler and H. Wahn, *Chest*, 2002, **121**, 573–581.
8 E. Malle, T. Buch and H. J. Grone, *Kidney Int.*, 2003, **64**, 1956–1967.
9 J. Perez-Vilar and R. C. Boucher, *Free Radicals Biol. Med.*, 2004, **37**, 1564–1577.
10 J. K. Andersen, *Nat. Med.*, 2004, **10**, S18–S25.
11 N. Güngör, A. M. Knaapen, A. Munnia, M. Peluso, G. R. Haenen, R. K. Chiu, R. W. L. Godschalk and F. J. van Schooten, *Mutagenesis*, 2010, **25**, 149–154.
12 (*a*) K. Setsukinai, Y. Urano, K. Kakinuma, H. J. Majima and T. Nagano, *J. Biol. Chem.*, 2003, **278**, 3170–3175; (*b*) S. Kenmoku, Y. Urano, H. Kojima and T. Nagano, *J. Am. Chem. Soc.*, 2007, **129**, 7313–7318; (*c*) Y. Koide, Y. Urano, S. Kenmoku, H. Kojima and T. Nagano, *J. Am. Chem. Soc.*, 2007, **129**, 10324–10325; (*d*) X. Chen, X. Wang, S. Wang, W. Shi, K. Wang and H. Ma, *Chem.–Eur. J.*, 2008, **14**, 4719–4724; (*e*) Z.-N. Sun, F.-Q. Liu, Y. Chen, P. K. H. Tam and D. Yang, *Org. Lett.*, 2008, **10**, 2171–2174; (*f*) W. Lin, L. Long, B. Chen and W. Tan, *Chem.–Eur. J.*, 2009, **15**, 2305–2309; (*g*) Y.-K. Yang, H. J. Cho, J. Lee, I. Shin and J. Tae, *Org. Lett.*, 2009, **11**, 859–861; (*h*) X. Q. Zhan, J. H. Yan, J. H. Su, Y. C. Wang, J. He, S. Y. Wang, H. Zheng and J. G. Xu, *Sens. Actuators, B*, 2010, **150**, 774–780; (*i*)

T.-I. Kim, S. Park, Y. Choi and Y. Kim, *Chem.–Asian J.*, 2011, **6**, 1358–1361; (*j*) Y. Koide, Y. Urano, K. Hanaoka, T. Terai and T. Nagano, *J. Am. Chem. Soc.*, 2011, **133**, 5680–5682; (*k*) X. Chen, K.-A. Lee, E.-M. Ha, K. M. Lee, Y. Y. Seo, H. K. Choi, H. N. Kim, M. J. Kim, C.-S. Cho, S. Y. Lee, W.-J. Lee and J. Yoon, *Chem. Commun.*, 2011, **47**, 4373–4375; (*l*) Y. Yang, Q. Zhao, W. Feng and F. Li, *Chem. Rev.*, 2013, **113**, 192–270; (*m*) Z. Lou, P. Li, Q. Pan and K. Han, *Chem. Commun.*, 2013, **49**, 2445–2447; (*n*) H. Zhu, J. Fan, J. Wang, H. Mu and X. Peng, *J. Am. Chem. Soc.*, 2014, **136**, 12820–12823; (*o*) L. Wang, L. Long, L. Zhou, Y. Wu, C. Zhang, Z. Han, J. Wang and Z. Da, *RSC Adv.*, 2014, **4**, 59535–59540; (*p*) Q. Xu, C. H. Heo, G. Kim, H. W. Lee, H. M. Kim and J. Yoon, *Angew. Chem., Int. Ed.*, 2015, **54**, 4890–4894; (*q*) L. Yuan, L. Wang, B. K. Agrawalla, S. J. Park, H. Zhu, B. Sivaraman, J. Peng, Q. H. Xu and Y. T. Chang, *J. Am. Chem. Soc.*, 2015, **137**, 5930–5938; (*r*) W. Zhang, W. Liu, P. Li, J. Kang, J. Wang, H. Wang and B. Tang, *Chem. Commun.*, 2015, **51**, 10150–10153; (*s*) Z. Zhang, C. Deng, L. Meng, Y. Zheng and X. Yan, *Anal. Methods*, 2015, **7**, 107–114; (*t*) J. J. Hu, N.-K. Wong, Q. Gu, X. Bai, S. Ye and D. Yang, *Org. Lett.*, 2014, **16**, 3544–3547; (*u*) J. Zhou, L. Li, W. Shi, X. Gao, X. Li and H. Ma, *Chem. Sci.*, 2015, **6**, 4884–4888.

13 A comparison of the performance of recently published fluorescent probes for HOCl imaging in terms of selectivity and sensitivity can be found in Table S2 of ESI.†

14 (*a*) D. Yang, H.-L. Wang, Z.-N. Sun, N.-W. Chung and J.-G. Shen, *J. Am. Chem. Soc.*, 2006, **128**, 6004–6005; (*b*) Z.-N. Sun, F.-Q. Liu, Y. Chen, P. K. H. Tam and D. Yang, *Org. Lett.*, 2008, **10**, 2171–2174; (*c*) Z.-N. Sun, H.-L. Wang, F.-Q. Liu, Y. Chen, P. K. H. Tam and D. Yang, *Org. Lett.*, 2009, **11**, 1887–1890; (*d*) T. Peng and D. Yang, *Org. Lett.*, 2010, **12**, 4932–4935; (*e*) J. J. Hu, N.-K. Wong, Q. Gu, X. Bai, S. Ye and D. Yang, *Org. Lett.*, 2014, **16**, 3544–3547; (*f*) T. Peng, N. K. Wong, X. Chen, Y. K. Chan, D. H. Ho, Z. Sun, J. J. Hu, J. Shen, H. El-Nezami and D. Yang, *J. Am. Chem. Soc.*, 2014, **136**, 11728–11734; (*g*) J. J. Hu, N.-K. Wong, S. Ye, X. Chen, M.-Y. Lu, A. Q. Zhao, Y. Guo, A. C.-H. Ma, A. Y.-H. Leung, J. Shen and D. Yang, *J. Am. Chem. Soc.*, 2015, **137**, 6837–6843.

15 E. K. Park, H. S. Jung, H. I. Yang, M. C. Yoo, C. Kim and K. S. Kim, *Inflammation Res.*, 2007, **56**, 45–50.

16 (*a*) D. I. Pattison and M. J. Davies, *Chem. Res. Toxicol.*, 2001, **14**, 1453–1464; (*b*) P. Nagy and M. T. Ashby, *Chem. Res. Toxicol.*, 2005, **18**, 919–923; (*c*) D. I. Pattison and M. J. Davies, *Curr. Med. Chem.*, 2006, **13**, 3271–3290.

17 (*a*) D. J. Rader and A. Daugherty, *Nature*, 2008, **451**, 904–913; (*b*) N. Zhang, K. P. Francis, A. Prakash and D. Ansaldi, *Nat. Med.*, 2013, **19**, 500–505; (*c*) M. A. Friese, B. Schattling and L. Fugger, *Nat. Rev. Neurol.*, 2014, **10**, 225–238.

18 (*a*) M. O. Crowhurst, J. E. Layton and G. J. Lieschke, *Int. J. Dev. Biol.*, 2002, **46**, 483–492; (*b*) A. C. Ma, T. K. Fung, R. H. Lin, M. I. Chung, D. Yang, S. C. Ekker and A. Y. Leung, *Blood*, 2011, **118**, 5448–5457.